Health-Aware control of an Octorotor UAV system based on actuator reliability

Jean C. Salazar, Adrián Sanjuan, Fatiha Nejjari and Ramon Sarrate
Research Center for Supervision, Safety and Automatic Control (CS2AC)
Universitat Politècnica de Catalunya, 10 Rambla Sant Nebridi, Terrassa, Spain
Email: jean.salazar@upc.edu

***Abstract*—A major goal in modern flight control systems is the need of improving the reliability. This work presents a reliable control approach of an octorotor UAV that allows distributing the control effort among the actuators using health actuator information. The octorotor is an over-actuated system where the redundancy of the actuators allows the redistribution of the control effort among the existing actuators according to a given control strategy. The priority is given to each actuator according to the capabilities and reliability of this actuator.**

***Keywords*—Prognosis and Health Management, UAV, Health-Aware Control, Reliability**

I. Introduction

Unmanned aerial vehicles (UAVs) are well-suited to a wide range of mission scenarios, such as search, rescue, vigilance and inspection, among others. However, the overall mission performance can be strongly influenced by vehicle sensors and actuators failures or degradations.

Moreover, for these kind of systems it could be more appropriate to avoid the fault occurrence than tolerate them. In this sense, a new paradigm in which the use of both control and reliability theory has emerged in terms of Health-Aware Control (HAC).

The aim is to modify the control inputs or change the mission objective, using system reliability information that is provided by a proper on-line prognostic tool. This leads to an increase of the operation time of the system [1, 2].

This work presents the benefit of taking into account system and component reliabilities in a linear quadratic control (LQR) algorithm of an overactuated system. In this kind of systems, the existence of some actuator redundancies allows the design of controllers that can optimise the distribution of the control effort in such a way that the reliability of the system is preserved or even extended. The objective is to combine a deterministic part related to the system dynamics and a stochastic part related to system reliability. The resulting scheme provides control performance and preserves the system reliability.

In particular, multirotors UAVs as overactuated systems have the potential to improve safety and reliability. Several control techniques have been applied to multirotors, such as Model Predictive Control (MPC) [3, 4, 5], PID [6] and LQR [7, 8]. Some control techniques have been used to design HAC strategies, i.e. with MPC [9] or control allocation [10].

The case study is an octorotor UAV system that has eight propellers in I configuration (Fig. 1). Four propellers can rotate in a clockwise direction, while the remaining can rotate anticlockwisely. The octorotor is moved by changing the rotor speeds. For example, increasing or decreasing together the eight propellers speeds, vertical motion is achieved. Changing only the speeds of the propellers situated oppositely produces either roll or pitch rotation, coupled with the corresponding lateral motion. Finally, yaw rotation results from the difference in the counter-torque between each pair of propellers. Moreover, the octorotor is an overactuated system which can function with at least four propellers forming a quadrotor structure.

The subsequent sections are as follows: in Section II the octorotor dynamics is presented, in Section III the reliability modelling is presented, in Section IV the dependence on system reliability in the control algorithm is discussed, in Section V the simulation results are presented, and finally, some conclusions are given in Section VI.

II. Octorotor Dynamics

To describe the dynamics of a multirotor, it is necessary to define the two frames in which it will operate: Inertial frame and Body frame. The inertial frame $\{\mathbf{I}\}$ is static and represents the reference of the multirotor while the body frame $\{\mathbf{B}\}$ is defined by the orientation of the multirotor and is situated in its center of mass. The two frames are related by the rotation matrix (1). $\mathbf{R}_C^I$ transforms a vector in body reference to a vector in inertial reference. In this case, the Euler angles, namely roll angle (ϕ), pitch angle (θ) and yaw angle (ψ), are used to model this rotation.

$$\mathbf{R}_C^I = \begin{bmatrix} c(\psi)c(\theta) & c(\psi)s(\theta)s(\phi) - s(\psi)c(\phi) & c(\psi)s(\theta)c(\phi) + s(\psi)s(\phi) \\ s(\psi)c(\theta) & s(\psi)s(\theta)s(\phi) + c(\psi)c(\phi) & s(\psi)s(\theta)c(\phi) - c(\psi)s(\phi) \\ -s(\theta) & c(\theta)s(\phi) & c(\theta)c(\phi) \end{bmatrix} \quad (1)$$

where $s(\cdot)$ and $c(\cdot)$ represent $\sin(\cdot)$ and $\cos(\cdot)$, respectively.

The dynamics of a multirotor [11] can be defined using the Newton and Euler equations (2)-(5), that describe the

This work was supported by Spanish Government (MINISTERIO DE ECONOMÍA Y COMPETITIVIDAD) and FEDER under project DPI2014-58104-R (HARCRICS).

translation and rotation of a rigid body.

$$\dot{\boldsymbol{\xi}}_I = \mathbf{v}_I \tag{2}$$

$$\dot{\mathbf{v}}_I = \frac{1}{m}(\mathbf{f}_I) \tag{3}$$

$$\dot{\boldsymbol{\eta}}_I = \mathbf{W}_\eta \boldsymbol{\omega}_B \tag{4}$$

$$\dot{\boldsymbol{\omega}}_B = \frac{1}{\mathbf{J}}(\boldsymbol{\tau}_B - \boldsymbol{\omega} \times \mathbf{J}\boldsymbol{\omega}) \tag{5}$$

where, $\boldsymbol{\xi}_I = [x\ y\ z]^T$ is the position vector, $\mathbf{v}_I = [v_x\ v_y\ v_z]^T$ is the linear speed vector in the inertial frame, $\boldsymbol{\eta} = [\phi\ \theta\ \psi]^T$ is the orientation vector, $\boldsymbol{\omega} = [p\ q\ r]^T$ is the body angular speed vector, m is the mass of the vehicle, $\mathbf{J}$ is the inertia tensor, $\mathbf{f}_I$ and $\boldsymbol{\tau}_B$ represent the external forces and torques applied to the UAV and $\mathbf{W}_\eta$ which represents the transformation matrix for angular velocities from the inertial frame to the body frame [12] is given by:

$$\mathbf{W}_\eta = \begin{bmatrix} 1 & \sin\phi\tan\theta & \cos\phi\tan\theta \\ 0 & \cos\phi & -\sin\phi \\ 0 & \dfrac{\sin\phi}{\cos\theta} & \dfrac{\cos\phi}{\cos\theta} \end{bmatrix} \tag{6}$$

The external forces interacting with the vehicle are: the lift of the rotors (T), the translational drag and the gravity. The external torques are: the motor torque (τ_m) and the rotational drag.

The model has been developed under the following assumptions [13]:

- The structure of the UAV is symmetrical.
- The body is rigid.
- The propellers are rigid.
- The free stream air velocity is zero.
- The motor dynamics is relatively fast and it can be neglected.
- The flexibility of the blade is relatively small and it can be neglected.
- The inertia tensor of the octorotor body is diagonal $\mathbf{J} = \text{diag}(J_{xx}, J_{yy}, J_{zz})$.
- The inertia of the octorotor body is much larger than the inertia of the propeller (it includes the rotating parts of the rotor) $\mathbf{J} \gg \mathbf{J}_{prop}$.
- Translational and rotational drag are negligible.

The multirotor model is obtained expanding the equations (2)-(5) and applying the previous assumptions:

$$\dot{x}_I = v_x \tag{7}$$

$$\dot{y}_I = v_y \tag{8}$$

$$\dot{z}_I = v_z \tag{9}$$

$$\dot{v}_x = \frac{1}{m}[\cos(\phi_I)\sin(\theta_I)\cos(\psi_I) + \sin(\phi_I)\sin(\psi_I)]T \tag{10}$$

$$\dot{v}_y = \frac{1}{m}[\cos(\phi_I)\sin(\theta_I)\sin(\psi_I) - \sin(\phi_I)\cos(\psi_I)]T \tag{11}$$

$$\dot{v}_z = \frac{1}{m}[\cos(\phi_I)\cos(\theta_I)]T - g \tag{12}$$

$$\dot{\phi}_I = p + \sin(\phi)\tan(\theta)q + \cos(\phi)\tan(\theta)r \tag{13}$$

$$\dot{\theta}_I = \cos(\phi)q - \sin(\phi)r \tag{14}$$

$$\dot{\psi}_I = \frac{\sin(\phi)}{\cos(\theta)}q + \frac{\cos(\phi)}{\cos(\theta)}r \tag{15}$$

$$\dot{p} = \frac{1}{J_{xx}}[-(J_{zz} - J_{yy})qr - J_p q\Omega_p + \tau_x] \tag{16}$$

$$\dot{q} = \frac{1}{J_{yy}}[(J_{zz} - J_{xx})pr + J_p p\Omega_p + \tau_y] \tag{17}$$

$$\dot{r} = \frac{1}{J_{zz}}[-(J_{yy} - J_{xx})pq + \tau_z] \tag{18}$$

where J_p is the inertia moment of the motor (rotating parts) and the propeller around z axis and T is the lift force.

Then, for the octorotor with the following structure PPNNPPNN as the one presented in Fig.1, where P and N define a positive and negative reactive motor torque respectively (represented as arrows), Ω_p is:

$$\Omega_p = -|\Omega_1| - |\Omega_2| + |\Omega_3| + |\Omega_4| - |\Omega_5| - |\Omega_6| + |\Omega_7| + |\Omega_8| \tag{19}$$

where Ω_i is the angular velocity of the ith motor.

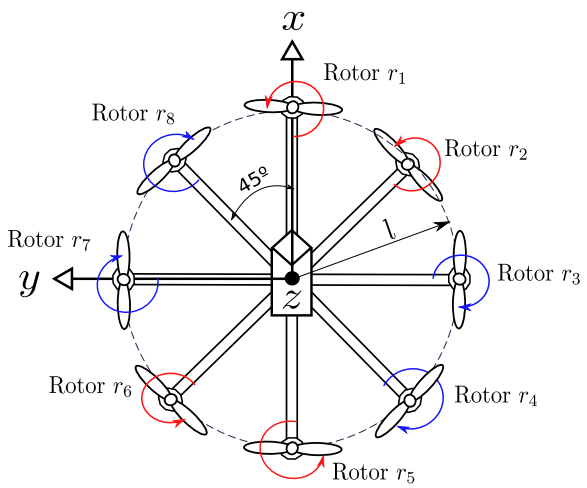

Fig. 1. Octorotor PPNNPPNN structure.

Furthermore, the system inputs Ω_i produce a lift force T and torques $\boldsymbol{\tau}$ in x, y, and z axis given by:

$$\mathbf{u}_v = \mathbf{B}_{str}\mathbf{u}_\Omega \tag{20}$$

which in its complete form is:

$$\begin{bmatrix} T \\ \tau_x \\ \tau_y \\ \tau_z \end{bmatrix} = \begin{bmatrix} k_b & k_b & k_b & k_b & k_b \\ 0 & -k_b l s(45) & -k_b l & -k_b l s(45) & 0 \\ -k_b l & -k_b l c(45) & 0 & +k_b l c(45) & k_b l \\ +k_d & +k_d & -k_d & -k_d & +k_d \end{bmatrix}$$

$$\begin{bmatrix} k_b & k_b & k_b \\ k_b ls(45) & k_b l & k_b ls(45) \\ k_b lc(45) & 0 & -k_b lc(45) \\ +k_d & -k_d & -k_d \end{bmatrix} \begin{bmatrix} \Omega_1^2 \\ \Omega_2^2 \\ \Omega_3^2 \\ \Omega_4^2 \\ \Omega_5^2 \\ \Omega_6^2 \\ \Omega_7^2 \\ \Omega_8^2 \end{bmatrix} \quad (21)$$

where k_b and k_d are coefficients of the motor and l is the distance between the center of mass and the center of the rotor. The parameters value which define the octorotor model are presented in Table I.

TABLE I. PARAMETERS VALUE

Parameter	Symbol	Value
Body inertia	$J_{xx} = J_{yy}$	$25 \cdot 10^{-3}$ $[kgm^2]$
Body inertia	J_{zz}	$42 \cdot 10^{-3}$ $[kgm^2]$
Propeller inertia	J_p	$104 \cdot 10^{-6}$ $[kgm^2]$
Mass	m	1.86 $[kg]$
Arm length	l	0.4 $[m]$
Thrust factor	k_b	$54.2 \cdot 10^{-6}$ $[Ns^2]$
Drag factor	k_d	$1.1 \cdot 10^{-6}$ $[Nms^2]$

Equations (7)-(18) define the non linear state space model of an octorotor that should be linearized to apply a health aware linear quadratic controller (LQR) for the UAV system. The state and inputs vectors considered are $\mathbf{x} = [x\ y\ z\ \phi\ \theta\ \psi\ v_x\ v_y\ v_z\ p\ q\ r]^T$ and $\mathbf{u} = [\Omega_1^2\ \Omega_2^2\ \Omega_3^2\ \Omega_4^2\ \Omega_5^2\ \Omega_6^2\ \Omega_7^2\ \Omega_8^2\ ]^T$, respectively, the Taylor series approximation at the hover position is applied. The hover position corresponds to the situation where the planes xy of both frames ($\{\mathbf{I}\}$ and $\{\mathbf{B}\}$) are in parallel and the motors are generating a lifting force equal to the weight of the octorotor.

In this work, the control of the UAV consists in a cascade structure (Fig. 2). Therefore, the linear model will be divided into two subsystems:

- For the inner control loop, let $\mathbf{e}_I$ be the inner state vector denoted as:

$$\mathbf{e}_I = \mathbf{X}_{ref_i} - \mathbf{X}_i = [e_z\ e_\phi\ e_\theta\ e_\psi\ e_{v_z}\ e_p\ e_q\ e_r]^T \quad (22)$$

and $\Delta\mathbf{u_I}$ be the inner input vector denoted as:

$$\Delta\mathbf{u_I} = \left[\Delta\Omega_1^2\ \Delta\Omega_2^2\ \Delta\Omega_3^2\ \Delta\Omega_4^2\ \Delta\Omega_5^2\ \Delta\Omega_6^2\ \Delta\Omega_7^2\ \Delta\Omega_8^2\right]^T \quad (23)$$

with $\Delta\Omega_i^2 = \Omega_i^2 - u_{ff} = \Omega_i^2 - mg/(8k_b)$, where u_{ff} stands for the input providing the equilibrium point.
Therefore, the inner loop model is given by:

$$\begin{aligned} \dot{\mathbf{e}}_I(t) =& \mathbf{A}_I\mathbf{e}_I(t) + \mathbf{B}_I\mathbf{B}_{str}\Delta\mathbf{u}_I(t) \\ \dot{\mathbf{e}}_I(t) =& \begin{bmatrix} \mathbf{0}_{4\times4} & \mathbf{I}_{4\times4} \\ \mathbf{0}_{4\times4} & \mathbf{0}_{4\times4} \end{bmatrix} \mathbf{e}_I(t) + \begin{bmatrix} \mathbf{0}_{4\times4} \\ \boldsymbol{\beta}_I \end{bmatrix} \mathbf{B}_{str}\Delta\mathbf{u}_I(t) \end{aligned} \quad (24)$$

where $\boldsymbol{\beta}_I = \text{diag}(1/m, 1/J_{xx}, 1/J_{yy}, 1/J_{zz})$ is a diagonal matrix, $\mathbf{I}_{4\times4}$ is the identity matrix and $\mathbf{B}_{str}$ is the structural matrix (21).

- For the outer control loop, let $\mathbf{e}_o$ be the outer state vector denoted as:

$$\mathbf{e}_o = \mathbf{X}_{ref_o} - \mathbf{X}_o = \left[e_x\ e_y\ e_{v_x}\ e_{v_y}\right]^T \quad (25)$$

and Δu_o be the outer input vector denoted as:

$$\Delta\mathbf{u}_o = [\Delta\phi\ \Delta\theta]^T = [\phi_{ref}\ \theta_{ref}]^T \quad (26)$$

Therefore, the outer loop model is:

$$\begin{aligned} \dot{\mathbf{e}}_o(t) =& \mathbf{A}_o\mathbf{e}_o(t) + \mathbf{B}_o\Delta\mathbf{u}_o(t) \\ \dot{\mathbf{e}}_o(t) =& \begin{bmatrix} \mathbf{0}_{2\times2} & \mathbf{I}_{2\times2} \\ \mathbf{0}_{2\times2} & \mathbf{0}_{2\times2} \end{bmatrix} \mathbf{e}_o(t) + \begin{bmatrix} 0 & 0 \\ 0 & 0 \\ 0 & g \\ -g & 0 \end{bmatrix} \Delta\mathbf{u}_o(t) \end{aligned} \quad (27)$$

where g is the gravitational acceleration equal to 9.81 $[m/s^2]$.

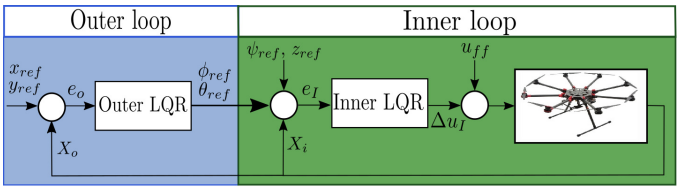

Fig. 2. Control scheme.

III. RELIABILITY MODELLING

Reliability is defined as the probability that units, components, equipment and systems will perform its functioning satisfactorily for a specified period of time under specified operating conditions and environments [14].

In particular, the reliability of the ith component of the system can be described by the exponential distribution as:

$$R_i(t) = e^{-\int_0^t \lambda_i(v)dv} \quad \forall\ i = 1, \ldots, m \quad (28)$$

where λ_i is the failure rate of the ith component. Several definitions of the failure rate can be found in the literature. In this work, the proportional hazard proposed by [15], is used:

$$\lambda_i(t) = \lambda_i^0 \cdot g(\ell, \vartheta) \quad \forall\ i = 1, \ldots, m \quad (29)$$

where λ_i^0 represents the nominal failure rate of the ith component and $g(\ell, \vartheta)$ is a load function also known as covariate which represents the effect of stress on the component failure rate as a function of the applied load (ℓ) and a component parameter (ϑ).

Different definitions of function $g(\ell, \vartheta)$ exists in the literature. In [16] the authors propose the load function based on the root-mean-square of the applied control input until the end of the mission (t_M), and an actuator parameter defined from the upper and lower saturation bound of u_i. This load function is used to distribute the control efforts between the redundant actuators, and the control action is calculated using a reliable state feedback controller.

In this work, the covariate is expressed as a function of the load and the age of the actuator:

$$g_i(u_i(t)) = 1 + \beta_i \int_0^t |u_i(v)|dv \quad \forall\ i = 1, \ldots, m \quad (30)$$

where $g_i(u_i(t))$ is defined as the cumulative applied control effort of the ith actuator from the beginning of the mission up to the current time t and β_i is a constant parameter.

Replacing (30) in (29) it yields,

$$\lambda_i(t) = \lambda_i^0 \left(1 + \beta_i \int_0^t |u_i(v)|dv\right) \quad \forall\ i = 1, \ldots, m \tag{31}$$

This definition implies that actuators are under a reliability decay due to the baseline failure rate which is increased when the actuators are used.

The overall system reliability can be computed by means of its structure function. The system structure function allows determining the system reliability based on their components and is determined by the structure of the system. It could be serial, parallel or a combination of both. In complex structures, i.e. bridge structure, it can be computed following the pivotal decomposition method [14]. Alternatively, system reliability can be modelled using a Dynamic Bayesian Network (DBN) [1].

In this work it is assumed that the overall system reliability is determined by the reliability of its actuators and the system controllability.

Although the octorotor system has 8 actuators ($r_i\ \forall\ i \in [1, 8]$) in terms of controllability, it can flight without any problem with at least 4 of them. In this case the system becomes a quadrotor. Among all 4-rotor configurations, the following minimal path sets which guarantee controllability can be found:

$$\begin{aligned} \zeta_1 &: \{r_1, r_3, r_5, r_7\} \\ \zeta_2 &: \{r_2, r_4, r_6, r_8\} \\ \zeta_3 &: \{r_2, r_3, r_6, r_7\} \\ \zeta_4 &: \{r_1, r_4, r_5, r_8\} \end{aligned} \tag{32}$$

Figure 3 presents the reliability block diagram based on the minimal path sets (ζ_i) where R_i is the ith rotor reliability.

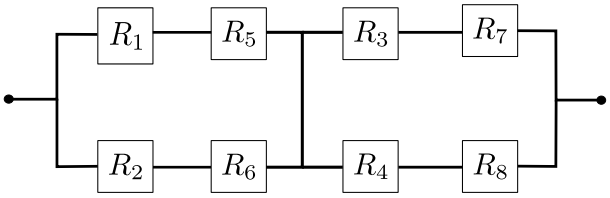

Fig. 3. Reliability block diagram.

Then the system reliability can be computed from the minimal path set by:

$$R_S = 1 - \prod_{j=1}^{4}(1 - R_{\zeta j}) \tag{33}$$

where $R_{\zeta j}$ is the reliability of the jth minimal path set, given by:

$$R_{\zeta j} = \prod_{i=k}^{l} R_i \quad \forall\ k, l \in \zeta_j \tag{34}$$

IV. Reliability based LQR Controller

A. LQR Controller

Consider the discrete-time, linear time-invariant (LTI) system,

$$\begin{cases} \mathbf{x}[k+1] = \mathbf{A}\mathbf{x}[k] + \mathbf{B}\mathbf{u}[k] \\ \mathbf{y}[k] = \mathbf{C}\mathbf{x}[k] \end{cases} \tag{35}$$

where $\mathbf{x} \in \mathbb{R}^{n_x}$ is the state vector, $\mathbf{u} \in \mathbb{R}^{n_u}$ is the input vector, $\mathbf{y} \in \mathbb{R}^{n_y}$ is the measurement vector, and $\mathbf{A} \in \mathbb{R}^{n_x \times n_x}$, $\mathbf{B} \in \mathbb{R}^{n_x \times n_u}$ and $\mathbf{C} \in \mathbb{R}^{n_y \times n_x}$ are the state, input and output matrix, respectively.

Given a cost function defined in a quadratic form,

$$J_{LQR} = \frac{1}{2}\sum_{k=0}^{\infty}\left(\mathbf{x}^T[k] \cdot \mathbf{Q} \cdot \mathbf{x}[k] + \mathbf{u}^T[k] \cdot \mathbf{R} \cdot \mathbf{u}[k]\right) \tag{36}$$

where $\mathbf{Q} \in \mathbb{R}^{n_x \times n_x}$ and $\mathbf{R} \in \mathbb{R}^{n_u \times n_u}$ are Hermitian positive definite. If the system is controllable and observable, a feedback control law can be defined as:

$$\mathbf{u}[k] = -\mathbf{K}\mathbf{x}[k] \tag{37}$$

where the optimal feedback gain ($\mathbf{K}$) is the solution of the cost function (36):

$$\mathbf{K} = (\mathbf{R} + \mathbf{B}^T\mathbf{P}\mathbf{B})^{-1}\mathbf{B}^T\mathbf{P}\mathbf{A} \tag{38}$$

The positive-definite symmetric matrix $\mathbf{P}$ is the solution of the discrete-time algebraic Riccati equation [17]:

$$\mathbf{P} = \mathbf{Q} + \mathbf{A}^T\mathbf{P}\mathbf{A} - \mathbf{A}^T\mathbf{P}\mathbf{B}(\mathbf{R} + \mathbf{B}^T\mathbf{P}\mathbf{B})^{-1}\mathbf{B}^T\mathbf{P}\mathbf{A} \tag{39}$$

B. Reliability

In this work, an approach based on the sensitivity of the system reliability to actuator reliability [18] (Birnbaum's measure) is used to tune the gain matrix $\mathbf{R}$ in the LQR cost function (36), in order to achieve a higher level of system reliability.

The system reliability sensitivity for the ith actuator is given by:

$$I_{Bi}(t) = \frac{\partial R_S(t)}{\partial R_i(t)} = R_S(1_i, t) - R_S(0_i, t) \tag{40}$$

where $R_S(1_i, t)$ denotes the system reliability where the ith actuator is perfectly reliable, and $R_S(0_i, t)$ denotes the system reliability when the ith actuator is faulty. This index indicates how sensitive is the system reliability against changes of a particular actuator reliability.

Thus, matrix $\mathbf{R}$ is modified at each sample time according to the system reliability sensitivity.

$$\mathbf{R}(t) = \text{diag}(I_B(t)) \tag{41}$$

For comparison purposes, an additional scenario will be considered, where no actuator reliability is taken into account in the LQR cost function. In this second scenario $\mathbf{R}$ will be set according to $\mathbf{R} = \mathbf{I}$ ($\mathbf{I}$ is the identity matrix of appropriate dimensions) and the corresponding system reliability will be denoted as $R_S^{\mathbf{I}}$ whereas the one obtained when $\mathbf{R}(t) = \text{diag}(I_B(t))$ will be denoted as $R_S^{I_B}$.

V. Simulation Results

The simulation consists in a corn field aerial supervision application. The corn field of $5000m^2$ is overflown by the octorotor at an altitude of $5m$ following the grid path and returning to the starting point presented in Fig. 4.

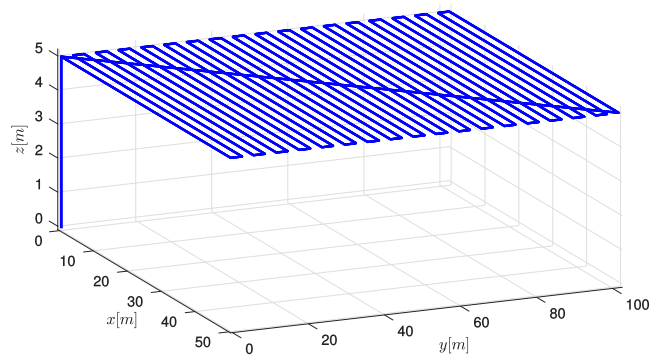

Fig. 4. UAV reference trajectory.

The simulation parameters are presented in Table II.

TABLE II. Simulation Parameters

Parameter	Symbol	Value
Outer sampling time	t_{si} $[s]$	0.05
Inner sampling time	t_{so} $[s]$	0.25
Simulation time	t_f $[s]$	2000
Rotor parameter	β_i	10^{-2} $\forall$ $i \in [1, 8]$
Rotors failure rate	λ_i^0	$\{21, 25, 2, 5, 16, 29, 9, 8\} \cdot 10^{-6}$ $[s^{-1}]$
Rotor upper bounds	$\overline{\mathbf{u}}_i$ $[N]$	7 $\forall$ $i \in [1, 8]$
Rotor lower bounds	$\underline{\mathbf{u}}_i$ $[N]$	0 $\forall$ $i \in [1, 8]$
Initial controlled outputs	$\mathbf{y}(0)$	0_x, 0_y, 0_z, 0_ψ
Initial states	$\mathbf{x}(0)$	$\mathbf{0}_{[12\times1]}$
Feed-Forward input	$\mathbf{u}_{ff}$	$mg/8_{[8\times1]}$

The tracking performance under both scenarios is almost identical. Figure 5 presents the tracking results of the LQR controller for the first 200 seconds in the scenario where $\mathbf{R}(t) = \text{diag}(I_B(t))$.

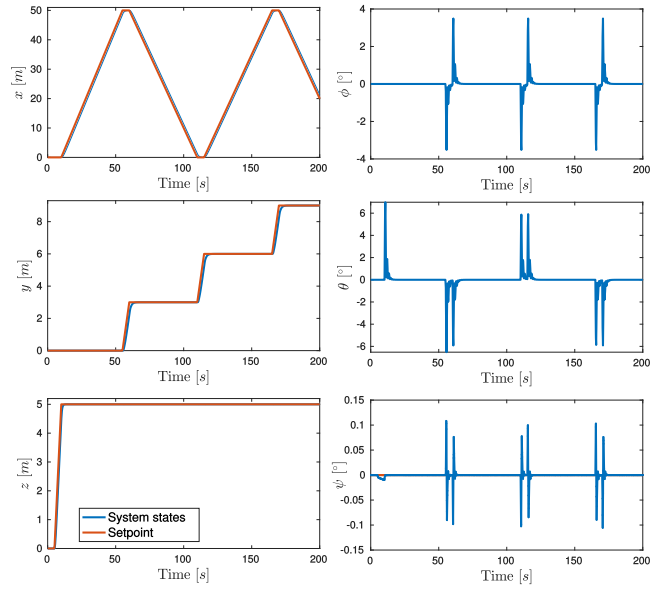

Fig. 5. System states response with $\mathbf{R}(t)$ =diag$(I_B(t))$.

However, $\mathbf{R}(t) = \text{diag}(I_B(t))$ preserves the critical rotors which cause a larger impact on the system reliability. Figure 6 shows the control efforts (angular velocities) in the scenarios where $\mathbf{R}(t) = \text{diag}(I_B(t))$ and $\mathbf{R}(t) = \mathbf{I}$ (i.e. $\Omega_i^{I_B}$, and Ω_i^I). The overall system reliability enhancement is achieved by relieving the control efforts of those rotors which are the most critical to the system. According to Fig. 6, this corresponds to rotors r_1, r_2, r_5 and r_6, which have a higher failure rate according to Table II, and cover all to the minimal path sets (see Fig. 3).

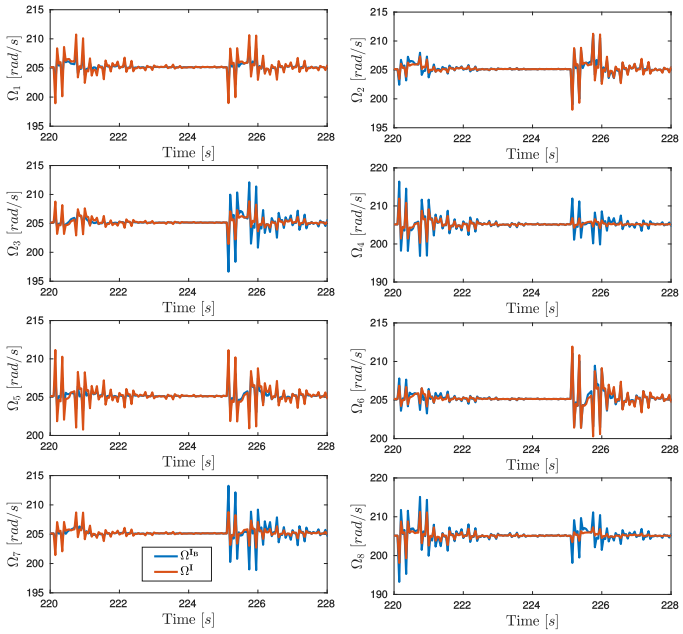

Fig. 6. Angular velocities $\Omega_i^{I_B}$ and Ω_i^I.

Figure 7 provides a comparison between the system reliability $R_S^{\mathbf{I}}$ and $R_S^{I_B}$ after having performed several missions. Under $\mathbf{R}(t) = \text{diag}(I_B(t))$, safety of the system is increased by allowing its operation until the end of the mission with a higher reliability level.

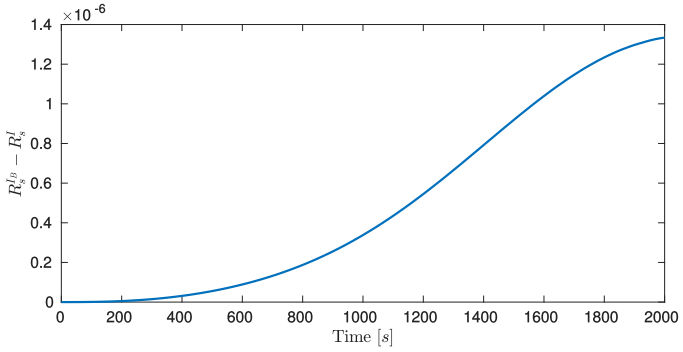

Fig. 7. Difference between system reliabilities $R_S^{I_B}$ and $R_S^{\mathbf{I}}$.

VI. Conclusion

In this work, an LQR tuning method based on the Birnbaum's reliability importance measure applied to an UAV octorotor is presented. The aim is to perform the control of the system and preserve its reliability by distributing the control

efforts among the actuators based on their importance to the system reliability. The tuning method uses the information about system and actuators reliabilities and their importance as a policy to adjust the gain matrix $\mathbf{R}$ accordingly.

As a key contribution, in this work the system reliability block diagram has been obtained from the system controllability analysis. At least 4 rotors are required to assure system controllability. Therefore, the minimal path sets have been determined based on those 4-rotor configurations that guarantee system controllability.

Simulation results demonstrates the validity of this approach in terms of reliability and controllability of the octorotor through an effective health management of the UAV actuators effort.

REFERENCES

[1] J. C. Salazar, P. Weber, F. Nejjari, D. Theilliol, and R. Sarrate, "MPC Framework for System Reliability Optimization," in *Advanced and Intelligent Computations in Diagnosis and Control*, ser. Advances in Intelligent Systems and Computing, Z. Kowalczuk, Ed. Springer International Publishing, 2015, no. 386, pp. 161–177.

[2] J. C. Salazar, F. Nejjari, R. Sarrate, P. Weber, and D. Theilliol, "Reliability importance measures for a health-aware control of drinking water networks," in *Proceedings of the 3rd Conference on Control and Fault-Tolerant Systems, SysTol 2016*, 2016.

[3] G. V. Raffo, M. G. Ortega, and F. R. Rubio, "An integral predictive/nonlinear control structure for a quadrotor helicopter," *Automatica*, vol. 46, no. 1.

[4] C. Liu, W.-H. Chen, and J. Andrews, "Tracking control of small-scale helicopters using explicit nonlinear MPC augmented with disturbance observers," *Control Engineering Practice*, vol. 20, no. 3, pp. 258–268, Mar. 2012.

[5] M. Abdolhosseini, Y. M. Zhang, and C. A. Rabbath, "An Efficient Model Predictive Control Scheme for an Unmanned Quadrotor Helicopter," *Journal of Intelligent & Robotic Systems*, vol. 70, no. 1-4, pp. 27–38, 2013.

[6] F. Rinaldi, A. Gargioli, and F. Quagliotti, "PID and LQ Regulation of a Multirotor Attitude: Mathematical Modelling, Simulations and Experimental Results," *Journal of Intelligent & Robotic Systems*, vol. 73, no. 1-4, pp. 33–50, 2014.

[7] A. Marks, J. Whidborne, and I. Yamamoto, "Control allocation for fault tolerant control of a VTOL octorotor," in *2012 UKACC International Conference on Control (CONTROL)*, 2012, pp. 357–362.

[8] V. G. Adîr and A. M. Stoica, "Integral LQR Control of a Star-Shaped Octorotor," *INCAS BULLETIN*, vol. 4, no. 2, pp. 3–18, 2012.

[9] J. C. Salazar, P. Weber, R. Sarrate, D. Theilliol, and F. Nejjari, "MPC design based on a DBN reliability model: Application to drinking water networks," in *Proceedings of the 9th IFAC Symposium on Fault Detection, Supervision and Safety for Technical Processes*, vol. 48, no. 21, Paris, France, 2015, pp. 688–693.

[10] A. Khelassi, J. Jiang, D. Theilliol, P. Weber, and Y. M. Zhang, "Reconfiguration of Control Inputs for Overactuated Systems Based on Actuators Health," in *Proceedings of the 18th IFAC World Congress, 2011*, Milano, Italy, 2011, pp. 13 729–13 734.

[11] R. Mahony, V. Kumar, and P. Corke, "Multirotor Aerial Vehicles: Modeling, Estimation, and Control of Quadrotor," *IEEE Robotics Automation Magazine*, vol. 19, no. 3, Sept. 2012.

[12] J. H. Blakelock, *Automatic Control of Aircraft and Missiles*. John Wiley & Sons, 1991.

[13] A. Freddi, A. Lanzon, and S. Longhi, "A Feedback Linearization Approach to Fault Tolerance in Quadrotor Vehicles," *IFAC Proceedings Volumes*, vol. 44, no. 1, pp. 5413–5418, 2011.

[14] I. B. Gertsbakh, *Reliability theory: with applications to preventive maintenance*, 2nd ed. Springer, 2001.

[15] D. R. Cox, "Regression Models and Life-Tables," *Journal of the Royal Statistical Society. Series B (Methodological)*, vol. 34, no. 2, pp. 187–220, Jan. 1972.

[16] A. Khelassi, D. Theilliol, P. Weber, and J.-C. Ponsart, "Fault-tolerant control design with respect to actuator health degradation: An LMI approach," in *Proceedings of the IEEE International Conference on Control Applications (CCA)*, 2011, pp. 983–988.

[17] K. Ogata, *Discrete-time Control Systems*, 2nd ed. Prentice - Hall Inc., 1987.

[18] Z. W. Birnbaum, "On the importance of different components in a multicomponent system," in *Multivariate analysis*, P. R. Krishnaiah, Ed. Academic Press, 1969, vol. II, pp. 581–592.